Frontiers in Bioscience Landmark

Front. Biosci. (Landmark Ed) **2025**; 30(8): 42710
https://doi.org/10.31083/FBL42710

Original Research

Requirement of Lysosomal Two-Pore Channels for Normal Fertilization and Artificial Oocyte Activation in Mice

Tadashi Yamazaki[1], Md Wasim Bari[2], Satoshi Kishigami[1,2,3,4,*]

[1]Department of Integrated Applied Life Science, Integrated Graduate School of Medicine, Engineering, and Agricultural Sciences, University of Yamanashi, 400-8510 Yamanashi, Japan
[2]Faculty of Life and Environmental Sciences, University of Yamanashi, 400-8510 Yamanashi, Japan
[3]Center for Advanced Assisted Reproductive Technologies, University of Yamanashi, 400-8510 Yamanashi, Japan
[4]Advanced Biotechnology Center, University of Yamanashi, 400-8510 Yamanashi, Japan
*Correspondence: skishigami@yamanashi.ac.jp (Satoshi Kishigami)
Academic Editor: Graham Pawelec
Submitted: 28 May 2025 Revised: 20 July 2025 Accepted: 30 July 2025 Published: 21 August 2025

Abstract

Background: Lysosomes serve not only in the degradation of cellular components but also as calcium (Ca^{2+}) stores. In this study, we investigated the effects of trans-Ned19, an inhibitor of lysosomal calcium channels known to block two-pore channels (TPCs), on fertilization and oocyte activation in mice. **Methods**: Pronuclear formation was assessed via Hoechst 33342 staining, cortical granule release was evaluated using *Lens culinaris* agglutinin-fluorescein isothiocyanate (LCA-FITC) staining, intracellular Ca^{2+} levels were monitored with Cal-520 AM, and sperm motility was analyzed using a sperm motility analysis system (SMAS). **Results**: In strontium (Sr^{2+})-induced oocyte activation, trans-Ned19 significantly reduced pronuclear formation at 8 h post-activation. Cortical granule release and Ca^{2+} oscillations were also markedly suppressed. In contrast, during *in vitro* fertilization (IVF), trans-Ned19 treatment significantly decreased the fertilization rate; however, pronuclear formation and cortical granule release remained comparable to controls in fertilized embryos. Notably, when IVF was performed using zona pellucida-free oocytes, the fertilization rate in the trans-Ned19 group was similar to that of the controls. However, a significant increase in polyspermy was observed. Furthermore, trans-Ned19 significantly impaired sperm motility parameters, including straight-line velocity, curvilinear velocity, and average path velocity. **Conclusions**: These findings suggest that lysosomal TPCs are essential for both normal fertilization and artificial oocyte activation in mice.

Keywords: calcium channels; *in vitro* fertilization; oocytes

1. Introduction

In mammals, mature oocytes are transformed into zygotes through fertilization with sperm. This process, known as oocyte activation, begins with a series of intracellular calcium (Ca^{2+}) oscillations, followed by events such as cortical granule release and pronuclear formation, ultimately leading to embryonic development [1,2]. During physiological oocyte activation, sperm-derived phospholipase C zeta (PLCζ) is known to trigger Ca^{2+} oscillations via activation of the inositol 1,4,5-trisphosphate (IP_3) receptor pathway [1]. Oocyte activation can also be artificially induced using methods such as electrical stimulation, ionophores, ethanol, and strontium (Sr^{2+}) [3]. However, the precise mechanisms underlying these activation methods remain unclear. Sr^{2+} has been reported to induce Ca^{2+} oscillations similar to those observed during fertilization, although several studies suggest mechanistic differences between Sr^{2+}-induced and sperm-induced activation [4,5]. In our previous study, we found that chloroquine (CQ), an antimalarial drug, does not fundamentally inhibit sperm-induced oocyte activation but does impair Sr^{2+}- and ethanol-induced activation by disrupting Ca^{2+} oscillations [6]. This result supports the notion that Sr^{2+} activates oocytes via a mechanism distinct from that of sperm. Given that CQ affects lysosomal function [7,8], we hypothesized that its effects on oocyte activation might be mediated through lysosomes.

Lysosomes not only function as degradative organelles for intra- and extracellular components but also serve as intracellular Ca^{2+} stores [9,10]. They interact with other calcium-regulating organelles, such as the endoplasmic reticulum and mitochondria, thereby modulating cytoplasmic Ca^{2+} signaling [11,12]. Lysosomal membranes harbor calcium -permeable two-pore channels (TPCs), which play a key role in regulating intracellular Ca^{2+} dynamics [13]. The animal TPC family comprises three subtypes: TPC1, TPC2, and TPC3 [14]. In humans and mice, only TPC1 and TPC2 are expressed, with distinct subcellular localizations-TPC1 is distributed across various endolysosomal compartments, whereas TPC2 is predominantly localized to late endosomes and lysosomes [15]. TPCs are activated by nicotinic acid adenine dinucleotide phosphate (NAADP) [16]. And the NAADP-TPC pathway has been implicated in fertilization. For example, TPC knockdown in sea star oocytes disrupts embryonic development due to impaired Ca^{2+} signaling [17]. In mice, NAADP-mediated Ca^{2+} signaling via TPC1 regulates the

acrosome reaction in sperm, and the presence of NAADP synthase has also been reported in human sperm [18–20]. Nonetheless, the role of TPCs in mammalian fertilization and oocyte activation remains largely unexplored.

Trans-Ned19 is a selective antagonist of NAADP and effectively inhibits NAADP-induced Ca^{2+} release [21]. Its inhibitory activity has been characterized across a broad concentration range, from 1 µM to 300 µM [21,22].

In this study, we investigated the potential involvement of TPC-mediated Ca^{2+} signaling in fertilization and oocyte activation using the NAADP antagonist trans-Ned19.

2. Materials and Methods

2.1 Animals

Institute of Cancer Research (ICR) female mice aged 8 weeks or older and ICR male mice aged 10 weeks or older were used. Mice were purchased from SLC (Japan SLC, Inc., Shizuoka, Japan) and bred in-house. They were maintained in a specific pathogen-free facility under controlled conditions (25 °C, 50% humidity, 14 h light/10 h dark cycle). Standard pelleted food and water were provided *ad libitum*. All animal procedures were approved by the Animal Experimentation Committee (protocol number A4-10) at the University of Yamanashi, Japan, and were conducted in accordance with ethical guidelines. Animal handling and experimentation adhered to the 3Rs principle and followed the Guidelines for Proper Conduct of Animal Experiments (Science Council of Japan).

2.2 Oocyte Collection

Female mice aged 8 weeks or older were administered 7.5 IU of pregnant mare serum gonadotropin (Aska Pharmaceutical, Tokyo, Japan) via intraperitoneal injection, followed 48 h later by 7.5 IU of human chorionic gonadotropin (hCG; Aska Pharmaceutical). Cumulus-oocyte complexes (COCs) were collected from the oviducts approximately 16 h after the hCG injection. All mice used in this study were euthanized by cervical dislocation.

2.3 In Vitro Fertilization (IVF) and Sr^{2+}-Induced Oocyte Activation With Trans-Ned19 Treatment

For IVF, sperm collected from the caudal epididymis of male mice aged 10 weeks or older were pre-incubated in a 100 µL droplet of human tubal fluid (HTF) medium at 37 °C and 5% (v/v) CO_2 for 1 h to induce capacitation (**Supplementary Table 1**). Subsequently, COCs and capacitated sperm were co-incubated in a 100 µL droplet of HTF medium at a final sperm concentration of 1.0×10^6 sperm/mL for 8 h.

For Sr^{2+}-induced oocyte activation, COCs were transferred to a 100 µL droplet of HEPES-buffered Chatot-Ziomek-Bavister (CZB) medium containing 0.1% (w/v) bovine testicular hyaluronidase (Sigma-Aldrich, St. Louis, MO, USA) and incubated for 20 min (**Supplementary Table 2**). They were then moved to a 15 µL droplet of CZB medium and cultured for 1 h. Cumulus-free oocytes were further incubated in a 15 µL droplet of Ca^{2+}-free CZB medium containing 5 mM $SrCl_2$ (Fujifilm Wako Pure Chemical Corporation, Osaka, Japan) at 37 °C under 5% CO_2 for 8 h (**Supplementary Table 3**). When trans-Ned19 (Sigma-Aldrich) was used, it was added to both fertilization and activation media at a final concentration of 300 µM.

To observe pronuclear formation, activated oocytes or oocytes after IVF were incubated in CZB medium containing 1 µg/mL Hoechst 33342 (Sigma-Aldrich) for more than 10 min and observed using a fluorescence microscope (BZ-X710 or BZ-X800, Keyence, Osaka, Japan).

2.4 Observation of Cortical Granules

Oocytes were cultured in CZB medium containing 5 µg/mL *Lens culinaris* agglutinin-fluorescein isothiocyanate (LCA-FITC; Vector Laboratories, Newark, CA, USA) for at least 10 min following 2 h of Sr^{2+}-induced activation or insemination. They were observed at room temperature using a fluorescence microscope. Cortical granule release was evaluated visually based on fluorescent images.

2.5 Analysis of Calcium Oscillations

Before Sr^{2+}-induced activation, oocytes were pre-incubated in CZB medium containing 5 µM Cal-520 AM (AAT Bioquest, Pleasanton, CA, USA) for 1 h. Time-lapse imaging was then performed using a fluorescence microscope. When trans-Ned19 was used, it was added to the activation medium at a final concentration of 300 µM. During imaging, oocytes were maintained in an incubation chamber with 5% CO_2, a top heater set to 45 °C and a bath heater set to 41 °C. Imaging was conducted at 30-second intervals for 3 h. Calcium signals were analyzed by measuring the average pixel value in the cytoplasmic region using Python 3.11.2 (Python Software Foundation, https://www.python.org/) and the OpenCV image processing library (https://opencv.org/).

2.6 Analysis of Sperm Motility

After 1 h of capacitation in a 100 µL droplet of HTF medium, sperm were further incubated in HTF medium containing 300 µM trans-Ned19 for 2 h. Sperm motility was assessed at room temperature using a sperm motility analysis system (SMAS; DITECT, Tokyo, Japan) with its built-in analysis software.

2.7 Statistical Analysis

Statistical analyses were performed using the chi-square test or Fisher's exact test, depending on the expected frequencies in 2×2 contingency tables. The chi-square test was performed in Microsoft Excel (version 2507; Microsoft Corporation, Redmond, WA, USA) using the CHISQ.TEST function when all expected frequencies were ≥ 5. For lower expected values, Fisher's exact test (two-tailed) was per-

Table 1. Pronuclear formation rate 8 h after insemination or activation.

		No. of oocyte	MII	0PN with a spem	PN formed					
					Total (%)	1PN (%)	1PN like (%)	2PN (%)	3PN ≤ (%)	Others
IVF	ctrl	51	6 (12)[a]	0 (0)	45 (88)	3 (7)[a]	0 (0)	41 (91)	1 (2)	0 (0)
	Ned	90	24 (27)[b]	1 (1)	65 (72)	0 (0)[b]	0 (0)	62 (95)	3 (5)	0 (0)
Sr^{2+}	ctrl	49	0 (0)[a]	-	49 (100)	47 (96)[a]	0 (0)[a]	2 (4)	0 (0)	0 (0)
	Ned	49	17 (35)[b]	-	32 (65)	22 (69)[b]	7 (22)[b]	1 (3)	0 (0)	2 (6)
	Late Ned	50	0 (0)[a]	-	50 (100)	49 (98)[a]	0 (0)[a]	0 (0)	0 (0)	1 (2)

MII, metaphase II oocyte; 0PN, embryo with sperm but without expanded pronucleus; 1PN, embryo with one pronucleus; 1PN like, embryo showing fluorescence resembling a single unexpanded pronucleus; 2PN, embryo with two pronuclei; 3PN ≤, embryo with more than three pronuclei; Others, embryos showing fluorescence resembling unexpanded pronuclei, excluding "1PN like"; IVF, *in vitro* fertilization; Sr^{2+}, strontium. For both IVF and Sr^{2+}-induced activation, the control data (ctrl) partially overlap with those reported in our previous study. [a, b] Significant differences (Chi-square test or Fisher's exact test, $p < 0.05$). The experiment was performed in at least three independent replicates.

formed in Python 3.11.13 using the fisher_exact function from the scipy.stats module (version 1.16.0) on Google Colaboratory (Google LLC, Mountain View, CA, USA). For comparisons among three groups, Bonferroni correction was applied for multiple testing. A significance level of $p < 0.05$ was considered statistically significant.

3. Results

3.1 Effect of Trans-Ned19 Treatment on Pronuclear Formation

To examine the effect of trans-Ned19 on pronuclear formation, 300 µM trans-Ned19 was added to the insemination medium for IVF and the activation medium for Sr^{2+}-induced oocyte activation. Pronuclei were assessed by Hoechst 33342 staining 8 h after the onset of insemination or Sr^{2+}-induced activation. As a result, trans-Ned19 significantly decreased the fertilization rate during IVF, although pronuclear formation was observed in all fertilized embryos except one (Fig. 1A and Table 1). In contrast, during Sr^{2+}-induced oocyte activation, trans-Ned19 treatment significantly reduced the pronuclear formation rate. However, when trans-Ned19 was added 2 hours after the onset of Sr^{2+}-induced activation, pronuclei were observed in nearly all embryos (Fig. 1B and Table 1). Interestingly, the incidence of small and incompletely expanded pronuclei—classified as "1PN like"—was significantly increased (Fig. 1C and Table 1). These findings suggest that trans-Ned19 does not inhibit sperm-induced oocyte activation but rather interferes with fertilization. In contrast, trans-Ned19 strongly impairs Sr^{2+}-induced oocyte activation.

3.2 Effect of Trans-Ned19 Treatment on Release of Cortical Granules

Next, we examined cortical granule signals 2 h after the onset of insemination or activation. As a result, cortical granule signals were observed in all fertilized embryos during IVF, regardless of trans-Ned19 treatment (Fig. 2A and Table 2). In contrast, in Sr^{2+}-induced oocyte activation, embryos lacking cortical granule signals were observed in the trans-Ned19-treated group (Fig. 2B and Table 2). Additionally, there was a significant increase in embryos displaying small granule signals, which were distinct from the prominent cortical granule signals observed in the control group (Fig. 2B and Table 2). These small granule signals were rarely detected in the control group. These results indicate that trans-Ned19 does not affect cortical granule release during sperm-induced oocyte activation but suppresses it during Sr^{2+}-induced oocyte activation.

3.3 Effect of Trans-Ned19 Treatment on Ca^{2+} Oscillations

Trans-Ned19 inhibited cortical granule release, an event that occurs at an early stage of Sr^{2+}-induced oocyte activation. To further investigate whether Ca^{2+} oscillations—which occur earlier than cortical granule release and initiate oocyte activation—were induced, we monitored cytoplasmic Ca^{2+} levels using the fluorescent Ca^{2+} indicator Cal-520 AM. As a result, the number of embryos exhibiting an increase in cytoplasmic Ca^{2+} signals following Sr^{2+}-induced activation was significantly reduced in the trans-Ned19-treated group compared to the control group (Fig. 3). These findings indicate that trans-Ned19 inhibits the initiation step of Sr^{2+}-induced oocyte activation by suppressing Ca^{2+} oscillations.

3.4 Effect of Trans-Ned19 Treatment on Pronuclear Formation in Zona-Free IVF

Previously, we demonstrated that CQ significantly reduced the fertilization rate in IVF; however, when using oocytes with the zona pellucida removed, the fertilization rate was restored to the level of the control group [5]. Similarly, in this study, we found that while trans-Ned19 treatment did not significantly affect the pronuclear formation rate, it tended to reduce the fertilization rate in IVF. To investigate this further, IVF was performed using zona-free oocytes, and pronuclear formation was assessed 8 h later. In the trans-Ned19-treated group, the fertilization rate was comparable to that of the control group, indicating the re-

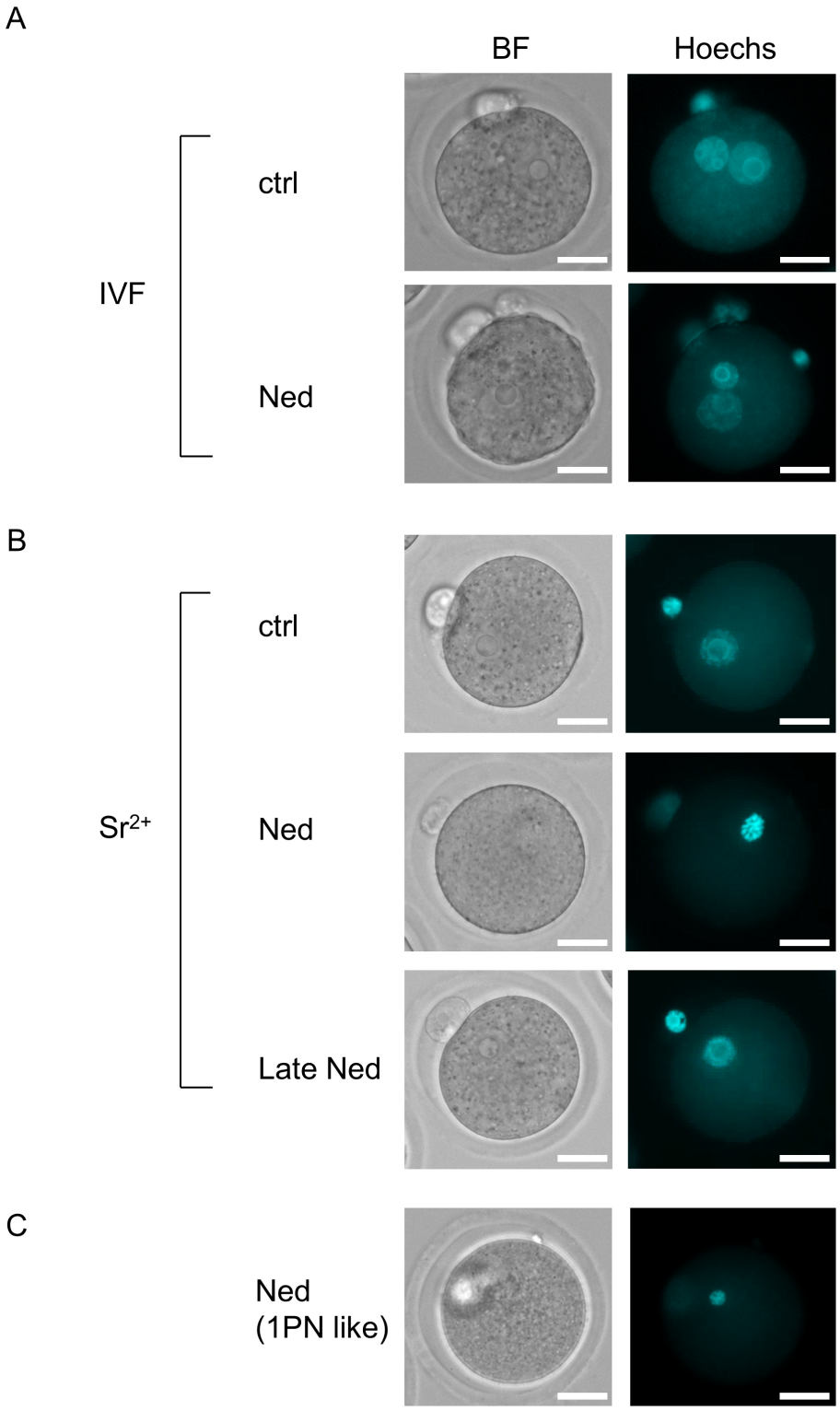

Fig. 1. Effects of trans-Ned19 on pronuclear formation after *in vitro* fertilization (IVF) and strontium (Sr^{2+})-induced activation. (A) Representative images showing pronuclear formation in trans-Ned19-untreated (control) and trans-Ned19-treated groups 8 h after IVF. Ctrl, trans-Ned19-untreated group; Ned, group treated with trans-Ned19 from the start of insemination. (B) Representative images of oocytes 8 h after Sr^{2+}-induced activation. Ctrl, trans-Ned19-untreated group; Ned, group treated with trans-Ned19 from the start of activation; Late Ned, group treated with trans-Ned19 starting 2 h after the onset of Sr^{2+}-induced activation. (C) "1PN like" embryo in the trans-Ned19-treated group after Sr^{2+}- induced activation. BF, bright-field image; Hoechst, fluorescence image stained with Hoechst 33342. Scale bar: 25 μm.

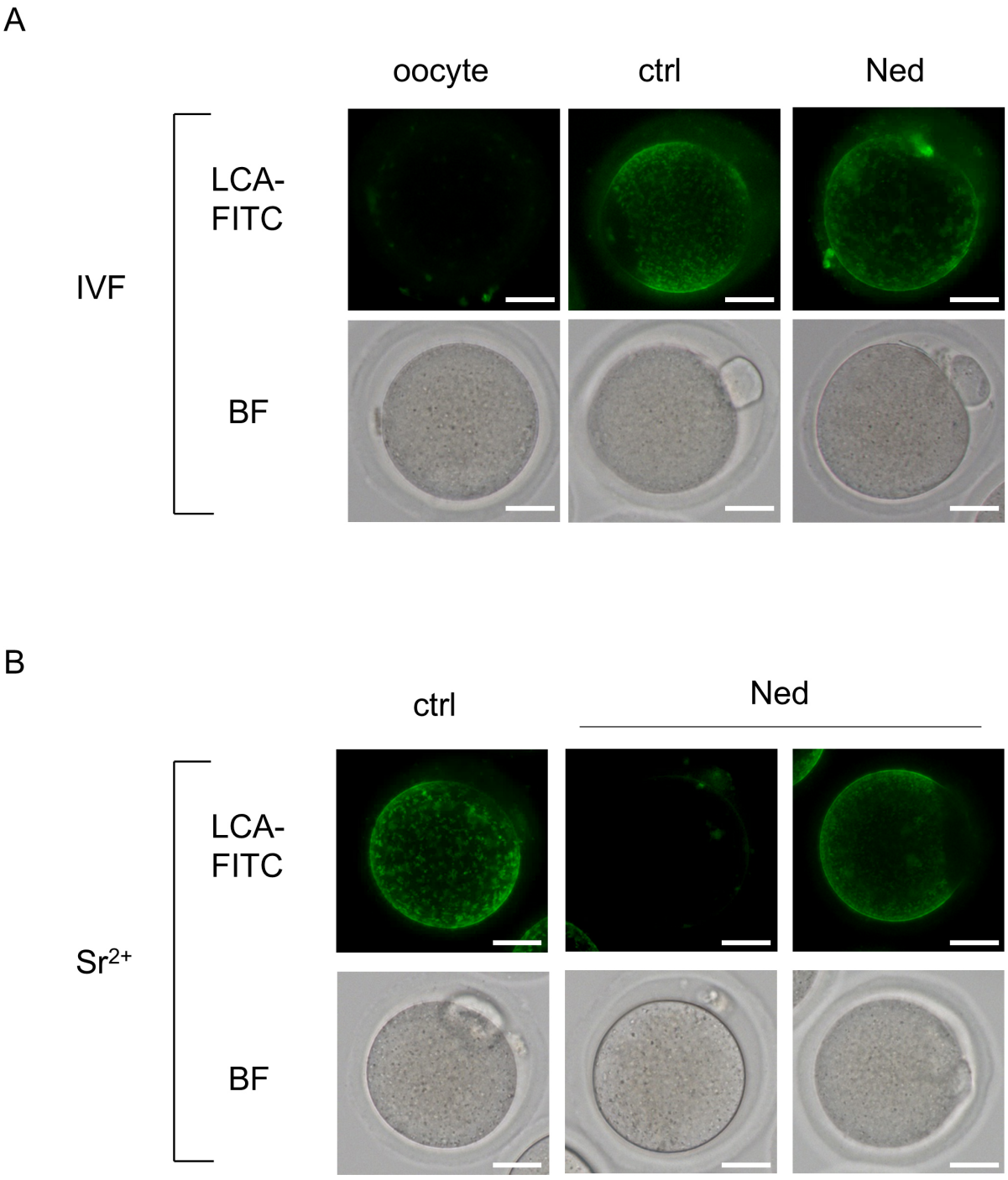

Fig. 2. *Lens culinaris* agglutinin-fluorescein isothiocyanate (LCA-FITC) staining results 2 h after IVF and Sr^{2+}-induced activation. (A) Results of IVF. Oocyte, metaphase II oocyte; Ctrl, trans-Ned19-untreated group; Ned, group treated with trans-Ned19 from the start of insemination. (B) Results of Sr^{2+}-induced activation. Oocyte, metaphase II oocyte; ctrl, trans-Ned19-untreated group; Ned, group treated with trans-Ned19 from the start of activation. For trans-Ned19-treated embryos during Sr^{2+}-induced activation, the left image shows an embryo without cortical granule release, and the right image shows an embryo with small granule signals. BF, bright field image. Scale bar: 25 µm.

moval of the zona pellucida restored fertilization competence. Expanded pronuclei were also observed, similar to those in the control group (Fig. 4 and Table 3). Notably, trans-Ned19 treatment significantly increased the number of embryos with more than three pronuclei (3PN $\leq$) (Table 3). These results suggest that trans-Ned19 reduces the fertilization rate by impairing sperm penetration through the zona pellucida and suppresses the oocyte's polyspermy-

Table 2. LCA-FITC signal 2 h after insemination or Sr^{2+}-induced activation.

		No. of oocyte	Fertilized (%)	LCA-FITC positive		
				Total (%)	Normal particles (%)	Small particles (%)
IVF	ctrl	46	38 (83)	38 (100)	38 (100)	0 (0)
	Ned	67	52 (78)	52 (100)	52 (100)	0 (0)
Sr^{2+}	ctrl	48	-	48 (100)[a]	47 (98)[a]	1 (2)[a]
	Ned	49	-	42 (86)[b]	26 (62)[b]	16 (38)[b]

Normal particles: normal *lens culinaris* agglutinin-fluorescein isothiocyanate (LCA-FITC) signal pattern; Small particles: small LCA-FITC signal pattern. In IVF, the percentage of fertilization was calculated based on the total number of oocytes tested (No. of oocyte), and the percentages of Normal particles and Small particles were calculated based on the number of fertilized embryos (Fertilized). In the case of Sr^{2+}-induced activation, the percentages of Normal particles and Small particles were calculated based on the total number of oocytes tested (No. of oocyte). For both IVF and Sr^{2+}-induced activation, the control data (ctrl) partially overlap with those reported in our previous study. [a, b] Significant differences (Chi-square test or Fisher's exact test, $p < 0.05$). The experiment was performed in at least three independent replicates.

Table 3. Pronuclear formation rate in IVF using zona-free oocytes.

	No. of oocyte	MII	1PN	2PN	3PN $\leq$
ctrl	47	0 (0)	3 (6)	37 (79)[a]	7 (15)[a]
Ned	56	1 (2)	3 (5)	25 (45)[b]	27 (48)[b]

MII, metaphase II oocyte; 1PN, embryo with one pronucleus; 2PN, embryo with two pronuclei; 3PN $\leq$, embryo with more than three pronuclei. The control data (ctrl) partially overlap with those reported in our previous study. [a, b] Significant differences (Chi-square test, $p < 0.05$). The experiment was performed in at least three independent replicates.

blocking mechanism.

3.5 Effect of Trans-Ned19 Treatment on Sperm Motility

Since trans-Ned19 reduced the fertilization rate by affecting sperm penetration through the zona pellucida, we examined whether trans-Ned19 treatment impairs sperm motility. Sperm were treated with trans-Ned19 for 2 h after capacitation, and their motility was subsequently assessed, as fertilization is considered to occur within 1–2 h after insemination under IVF conditions. As a result, trans-Ned19 treatment significantly reduced the proportion of sperm exhibiting high motility, as indicated by decreased straight-line velocity, curvilinear velocity, and average path velocity (Fig. 5). In addition, the proportion of immotile sperm was significantly increased, with a similar trend observed as early as 1 hour after trans-Ned19 treatment (data not shown). These findings suggest that the impaired passage of sperm through the zona pellucida is partly due to reduced motility caused by trans-Ned19 treatment.

4. Discussion

For oocyte activation, calcium is released from intracellular Ca^{2+} stores, primarily the endoplasmic reticulum (ER), through the activation of IP_3-gated Ca^{2+} release channels (IP_3 receptors) [1]. In animal cells, NAADP, another Ca^{2+}-mobilizing messenger, initiates Ca^{2+} release from the endolysosomal system via activation of TPCs [13]. However, the involvement of TPCs in oocyte activation remains unknown in mammals. In this study, we demonstrated that inhibition of TPCs by trans-Ned19 had little effect on sperm-induced oocyte activation, whereas it significantly suppressed Sr^{2+}-induced oocyte activation by inhibiting Ca^{2+} oscillations. These results suggest that the cascade of sperm-induced oocyte activation is distinct from that of Sr^{2+}-induced activation, consistent with our previous findings [6].

Although both TPC1 and TPC2 are present in mice [15], at least TPC1, which is localized to lysosomes and endosome, is expressed in mouse oocytes [23]. In sperm, TPC1 has been reported to localize to the acrosome and nuclear redundant vesicles [18]. Trans-Ned19, a selective and cell-permeant NAADP antagonist, is widely used to study the functional roles of TPCs [24]. In smooth muscle cells, 100 µM trans-NED 19 reduces TPC1-mediated Ca^{2+} elevation by nearly 60% [25]. In the present study, 300 µM trans-NED19 significantly suppressed Sr^{2+}-induced Ca^{2+} oscillations, leading to a failure of normal pronuclear formation in approximately 50% of embryos. In mice, Sr^{2+} influx—which induces Ca^{2+} oscillations and triggers oocyte activation—occurs via transient receptor potential vanilloid 3 (TRPV3) channels [26]. Therefore, it is reasonable to propose that increased intracellular Sr^{2+} may induce oocyte activation via Ca^{2+} release from lysosomes, likely through TPCs, either directly or indirectly. However, even under trans-Ned19 treatment, expanded pronuclei were observed in approximately 50% of embryos, suggesting that pronuclear formation during Sr^{2+}-induced activation is not solely dependent on TPC function. Consistently, it has been suggested that Sr^{2+} can sensitize IP_3 receptors and promote Ca^{2+} oscillations [5]. Furthermore, when trans-Ned19 was added 2 h after the start of Sr^{2+}-induced activation, it did not affect pronuclear formation. In mice, pronuclei are typ-

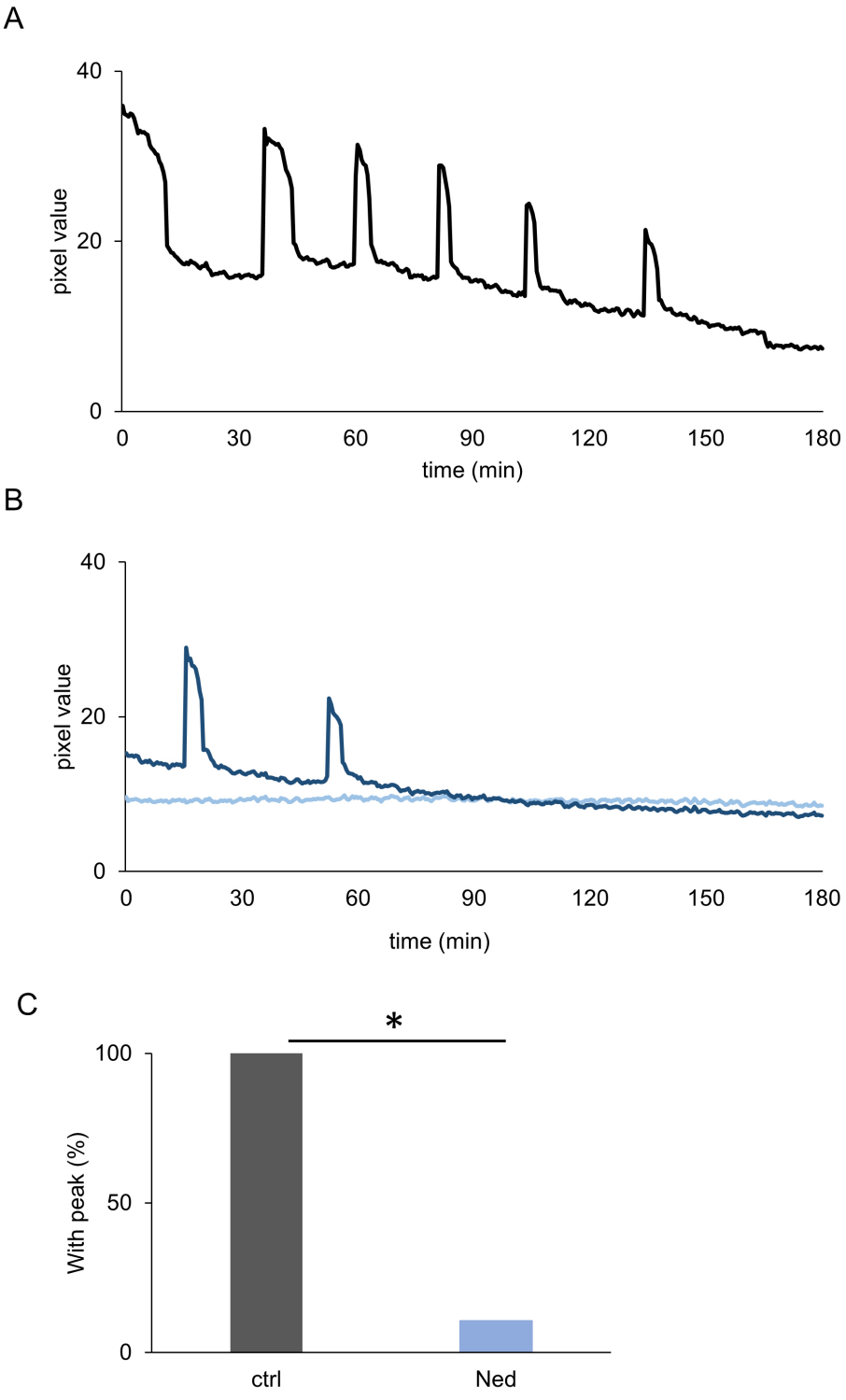

Fig. 3. Cytoplasmic calcium (Ca^{2+}) signal imaging results up to 3 h after the start of Sr^{2+}-induced activation. (A) Changes in pixel values within the embryonic cytoplasmic region in the trans-Ned19-untreated group. (B) Changes in pixel values within the embryonic cytoplasmic region in the trans-Ned19-treated group. In both (A,B), the horizontal axis represents time (min) from the start of imaging, and the vertical axis represents pixel value. The graphs show results from representative embryos. (C) Percentage of embryos showing an increase in pixel values in the trans-Ned19-untreated group (ctrl) and the trans-Ned19-treated group (Ned). The control data (ctrl) overlap with those reported in our previous study. *Significant differences (Chi-square test, $p < 0.05$). ctrl, n = 27; Ned, n = 28. The experiment was performed in at least three independent replicates.

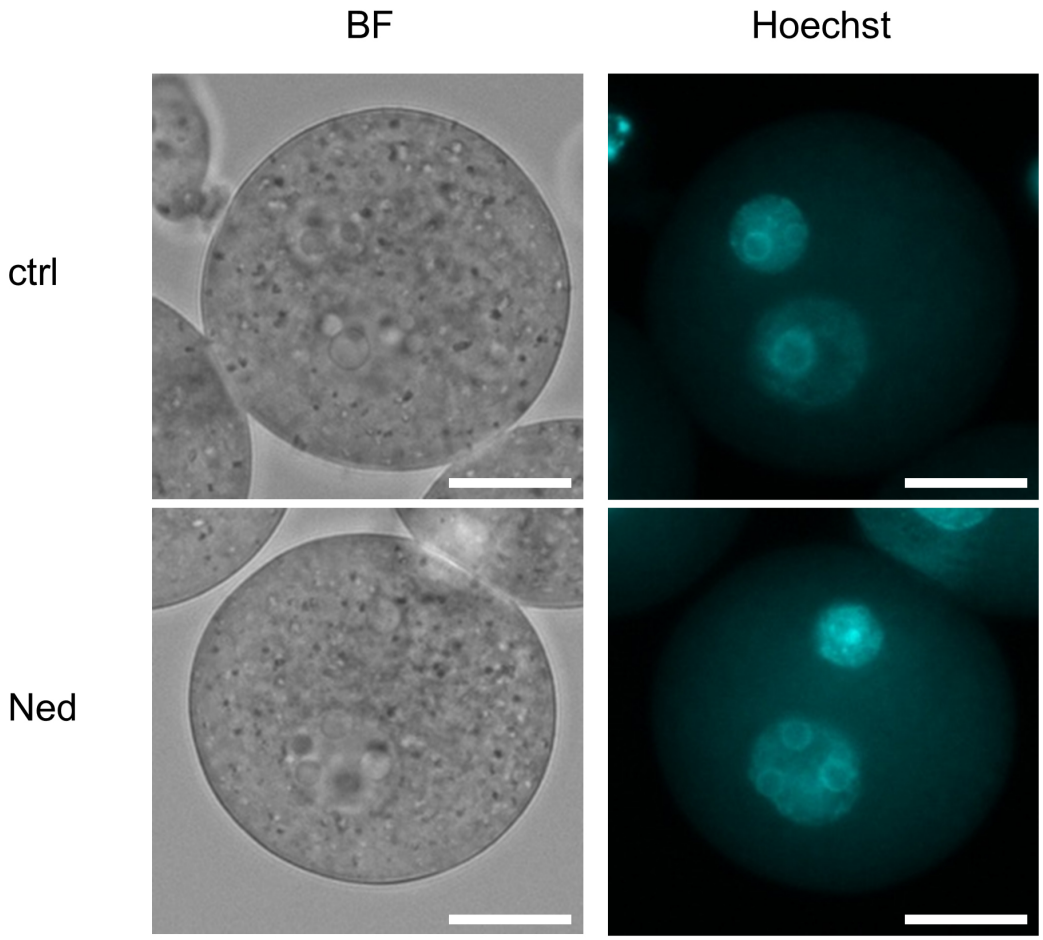

Fig. 4. Hoechst staining after 8 h after insemination using zona-free oocytes. Representative images showing pronuclear formation in the trans-Ned19-untreated and trans-Ned19-treated groups 8 h after zona-free IVF. Ctrl, trans-Ned19-untreated group; Ned, group treated with trans-Ned19 from the start of insemination; BF, bright-field image; Hoechst, fluorescent image stained with Hoechst 33342. Scale bar: 25 µm.

ically formed approximately 3 h after fertilization, suggesting that TPCs are not involved in the later stages of pronuclear formation [27].

In contrast, in IVF embryos, expanded pronuclei were observed in nearly all fertilized embryos, even under trans-Ned19 treatment. This suggests that lysosomal TPCs are not essential for sperm-induced oocyte activation. These findings support the notion that TPC1-mediated Ca^{2+} release contributes to Sr^{2+}-induced oocyte activation, whereas sperm-induced oocyte activation likely proceeds through a distinct Ca^{2+} signaling pathway independent of TPC1. Together, our results highlight mechanistic differences between artificial and physiological modes of oocyte activation and underscore the selective involvement of TPCs in non-physiological activation pathways.

Although trans-Ned19 treatment significantly reduced the fertilization rate in IVF, the rate became comparable to that in the control group after removal of the zona pellucida. Furthermore, trans-Ned19 treatment significantly decreased sperm motility, suggesting that TPCs in sperm may be required for maintaining normal motility. While the role of TPCs in sperm motility remains to be fully elucidated, Ca^{2+} signaling is known to regulate sperm motility, and inhibition of TPC-derived Ca^{2+} signaling by trans-Ned19 may contribute to the observed reduction [28]. In addition, TPCs have been reported to be involved in the regulating the acrosome reaction. Inhibition of TPCs by trans-Ned19 has been reported to impair the acrosome reaction in sperm, and a recent study suggests that this may occur via TPC-mediated Ca^{2+} signaling, potentially contributing to reduced fertilization rates [18,19].

Although trans-Ned19 has been widely used as a selective TPC inhibitor, its effects may not be entirely specific and can vary depending on the experimental context. While trans-Ned19 has been employed in numerous studies investigating NAADP-sensitive Ca^{2+} signaling, its specificity and potential off-target effects may differ depending on cell type, dosage, and exposure conditions. In the present study, we focused on identifying the potential involvement of TPCs in fertilization and oocyte activation

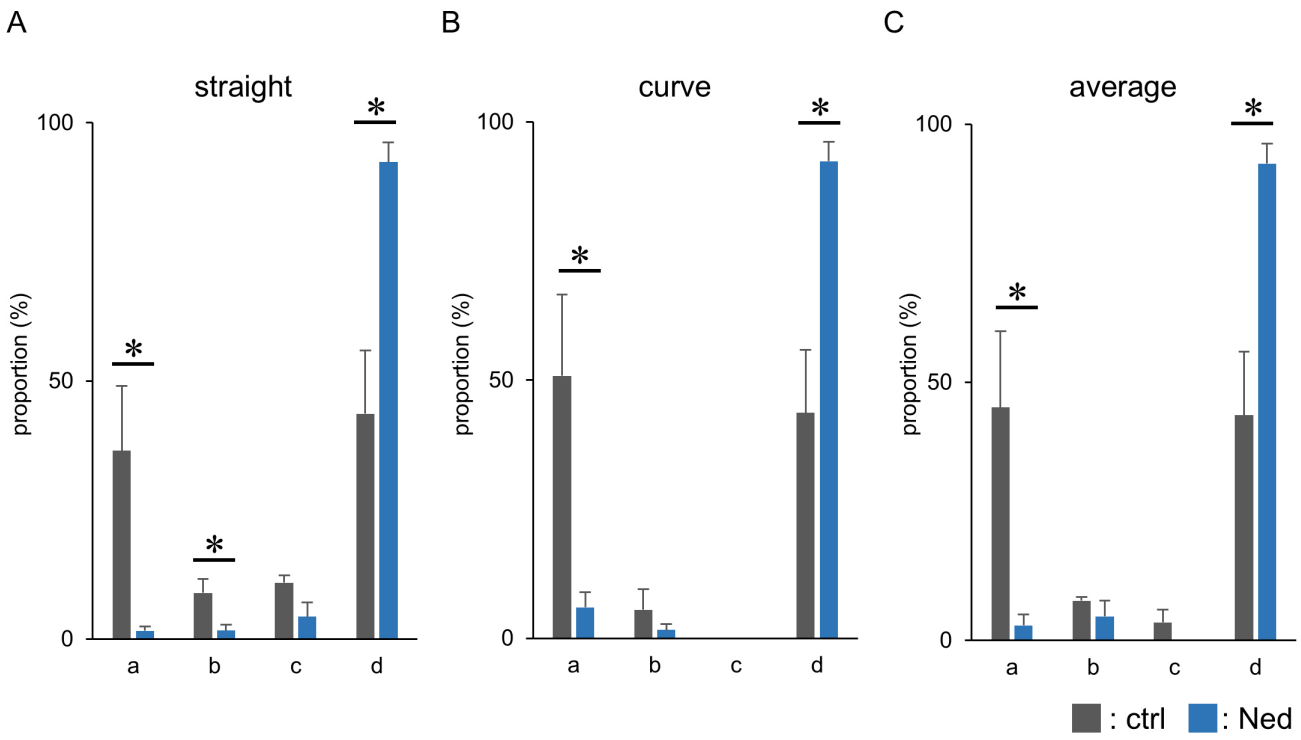

Fig. 5. Sperm motility distribution 2 h after trans-Ned19 treatment. (A–C) Graphs showing sperm motility characteristics measured 2 h after trans-Ned19 treatment. (A) Straight-line velocity; (B) curvilinear velocity; (C) average path velocity. In each graph, the horizontal axis (a–d) indicates velocity ranges: a: ≥25 µm/s, b: 5–25 µm/s, c: 0–5 µm/s, d: 0 µm/s (immotile). The vertical axis indicates the percentage of sperm within each velocity range. Data are presented as means + standard error of the mean (SEM). The control data (ctrl) overlap with those reported in previous study. *Significant differences (Chi-square test, $p < 0.05$). n ≥ 300 for each group. The experiment was performed in at least three independent replicates.

using trans-Ned19 as a pharmacological tool. However, we acknowledge the limitation of relying on a single inhibitor at a high concentration and recognize the need for further validation. Future studies incorporating additional pharmacological agents—such as SG-094, cis-Ned19, and TPC agonists (e.g., TPC2-A1-N and TPC2-A1-P)—will be essential to strengthen causal interpretation and expand upon the current findings.

On the other hand, the significantly increased incidence of polyspermy observed in zona-free IVF under trans-Ned19 treatment suggests that TPCs are involved in the mechanisms that prevent polyspermy in oocytes.

Rejection of polyspermy is known to occur at both the zona pellucida and the oocyte membrane, referred to as the "zona block" and "membrane block", respectively. In IVF using zona-free oocytes, the membrane block is considered the primary barrier to polyspermy [29]. Although this block is thought to be associated with the loss of the oocyte membrane protein IZUMO1 receptor, also known as folate receptor 4 (JUNO) following fertilization [30], the underlying mechanisms remain largely unclear. Since cortical granule release was observed even under trans-Ned19 treatment, it is suggested that TPC involvement in polyspermy prevention occurs mainly at the level of the oocyte membrane. Interestingly, an increase in cytosolic Ca^{2+} alone is not sufficient to establish the membrane block [18]. In normal fertilization, TPC-mediated activity may be required for the establishment of this membrane block. Future studies should aim to elucidate how TPCs contribute to this process.

Cortical granules undergo Ca^{2+}-dependent exocytosis, releasing their contents into the perivitelline space and modifying the zona pellucida to prevent polyspermy—a process known as the cortical reaction. This secretion mediated by the soluble NSF-attachment protein receptor (SNARE) protein pathway [31]. Trans-Ned19 treatment did not suppress cortical granule release in fertilized embryos, suggesting that TPC activity is not required for the cortical reaction during sperm-induced oocyte activation, consistent with its dispensability in pronuclear formation. In contrast, during Sr^{2+}-induced oocyte activation, trans-Ned19 treatment significantly decreased the number of embryos exhibiting normal granule signals and significantly increased those with small granule signals. This suggests that TPC function is required for normal cortical reactions in Sr^{2+}-induced activation. Even under trans-Ned19 treatment, 53% of embryos exhibited cortical granule release patterns similar to the control group, and the pronuclear formation rate was 47%, suggesting that some embryos suc-

cessfully completed cortical granule release but failed to form expanded pronuclei. Conversely, embryos with small granule signals may have failed to form pronuclei, indicating a correlation between the granule signal pattern and pronuclear formation. These observations suggest that incomplete activation signals under trans-Ned19 treatment result in abnormal cortical reactions and defective pronuclear formation.

5. Conclusions

Inhibition of TPCs by trans-Ned19 had minimal impact on sperm-induced oocyte activation during IVF, whereas Sr^{2+}-induced oocyte activation was inhibited from the initiation stage—specifically, at the onset of Ca^{2+} oscillations—leading to significant reductions in cortical granule release and pronuclear formation. Additionally, trans-Ned19 treatment was associated with a trend toward decreased sperm motility and fertilization rates, which were restored upon removal of the zona pellucida. These effects were similar to those observed with CQ treatment [6], suggesting that lysosome-derived Ca^{2+} signaling, including TPC-mediated pathways, may be a common target of both agents. More importantly, TPCs may contribute to the prevention of polyspermy, highlighting their role in post-fertilization events. Together, these findings provide new insights into the mechanisms of oocyte activation and hold potential implications for the advancement of assisted reproductive technologies.

Abbreviations

CQ, chloroquine; TPC, two-pore channel; NAADP, nicotinic acid adenine dinucleotide phosphate; IVF, *in vitro* fertilization.

Availability of Data and Materials

All raw data for this study are available from the corresponding author.

Author Contributions

TY and SK designed the research study. TY and MWB performed the experiments. SK provided guidance and support throughout the research. TY analyzed the data. TY and SK wrote the manuscript. All authors contributed to revisions of the manuscript, reviewed and approved the final version, and agreed to be accountable for all aspects of the work.

Ethics Approval and Consent to Participate

All the animal experiments were approved by the Animal Experimentation Committee at the University of Yamanashi, Japan, and conducted in accordance with the ethical guidelines (protocol number A4-10). Animal handling and experimentation adhered to the 3Rs principle and followed the Guidelines for Proper Conduct of Animal Experiments issued by the Science Council of Japan.

Acknowledgment

We gratefully acknowledge discussions and technical support with Dr. H. Harayama in Kobe University, Drs. T. Wakayama, S. Wakayama, D. Ito, and Ms. Y. Kanda at the Advanced Biotechnology Center, and also Ms. S. Furusato at the Center for advanced Assisted Reproductive Technologies, University of Yamanashi as well as all the lab members.

Funding

This work was supported by JSPS KAKENHI Grant (Numbers 20K06443 and 24K01937 to SK).

Conflict of Interest

The authors declare no conflict of interest.

Supplementary Material

Supplementary material associated with this article can be found, in the online version, at https://doi.org/10.31083/FBL42710.

References

[1] Amdani SN, Jones C, Coward K. Phospholipase C zeta (PLCζ): oocyte activation and clinical links to male factor infertility. Advances in Biological Regulation. 2013; 53: 292–308. https://doi.org/10.1016/j.jbior.2013.07.005.

[2] Sugita H, Takarabe S, Kageyama A, Kawata Y, Ito J. Molecular Mechanism of Oocyte Activation in Mammals: Past, Present, and Future Directions. Biomolecules. 2024; 14: 359. https://doi.org/10.3390/biom14030359.

[3] Versieren K, Heindryckx B, Lierman S, Gerris J, De Sutter P. Developmental competence of parthenogenetic mouse and human embryos after chemical or electrical activation. Reproductive Biomedicine Online. 2010; 21: 769–775. https://doi.org/10.1016/j.rbmo.2010.07.001.

[4] Sanders JR, Ashley B, Moon A, Woolley TE, Swann K. PLCζ Induced Ca^{2+} Oscillations in Mouse Eggs Involve a Positive Feedback Cycle of Ca^{2+} Induced $InsP_3$ Formation From Cytoplasmic PIP_2. Frontiers in Cell and Developmental Biology. 2018; 6: 36. https://doi.org/10.3389/fcell.2018.00036.

[5] Zhang D, Pan L, Yang LH, He XK, Huang XY, Sun FZ. Strontium promotes calcium oscillations in mouse meiotic oocytes and early embryos through InsP3 receptors, and requires activation of phospholipase and the synergistic action of InsP3. Human Reproduction (Oxford, England). 2005; 20: 3053–3061. https://doi.org/10.1093/humrep/dei215.

[6] Yamazaki T, Bari MW, Kishigami S. Chloroquine inhibits artificial oocyte activation induced by ethanol or Sr^{2+} but not by sperm in mice. Journal of Reproduction and Development. 2025; 71: 49–54. https://doi.org/10.1262/jrd.2024-089.

[7] Mauthe M, Orhon I, Rocchi C, Zhou X, Luhr M, Hijlkema KJ, *et al*. Chloroquine inhibits autophagic flux by decreasing autophagosome-lysosome fusion. Autophagy. 2018; 14: 1435–1455. https://doi.org/10.1080/15548627.2018.1474314.

[8] Fedele AO, Proud CG. Chloroquine and bafilomycin A mimic lysosomal storage disorders and impair mTORC1 signalling. Bioscience Reports. 2020; 40: BSR20200905. https://doi.org/10.1042/BSR20200905.

[9] Scott CC, Wasnik V, Nunes-Hassler P, Demaurex N, Kruse K, Gruenberg J. Calcium storage in multivesicular endo-lysosome.

Physical Biology. 2023; 20: 10.1088/1478–3975/acfe6a. https://doi.org/10.1088/1478-3975/acfe6a.

[10] Kang H, Choi SW, Kim JY, Oh SJ, Kim SJ, Lee MS. ER-to-lysosome Ca^{2+} refilling followed by K^{+} efflux-coupled store-operated Ca^{2+} entry in inflammasome activation and metabolic inflammation. eLife. 2024; 12: RP87561. https://doi.org/10.7554/eLife.87561.

[11] Atakpa P, Thillaiappan NB, Mataragka S, Prole DL, Taylor CW. IP_3 Receptors Preferentially Associate with ER-Lysosome Contact Sites and Selectively Deliver Ca^{2+} to Lysosomes. Cell Reports. 2018; 25: 3180–3193.e7. https://doi.org/10.1016/j.celrep.2018.11.064.

[12] Peng W, Wong YC, Krainc D. Mitochondria-lysosome contacts regulate mitochondrial Ca^{2+} dynamics via lysosomal TRPML1. Proceedings of the National Academy of Sciences of the United States of America. 2020; 117: 19266–19275. https://doi.org/10.1073/pnas.2003236117.

[13] Calcraft PJ, Ruas M, Pan Z, Cheng X, Arredouani A, Hao X, *et al*. NAADP mobilizes calcium from acidic organelles through two-pore channels. Nature. 2009; 459: 596–600. https://doi.org/10.1038/nature08030.

[14] Brailoiu E, Churamani D, Cai X, Schrlau MG, Brailoiu GC, Gao X, *et al*. Essential requirement for two-pore channel 1 in NAADP-mediated calcium signaling. The Journal of Cell Biology. 2009; 186: 201–209. https://doi.org/10.1083/jcb.200904073.

[15] Ruas M, Chuang KT, Davis LC, Al-Douri A, Tynan PW, Tunn R, *et al*. TPC1 has two variant isoforms, and their removal has different effects on endo-lysosomal functions compared to loss of TPC2. Molecular and Cellular Biology. 2014; 34: 3981–3992. https://doi.org/10.1128/MCB.00113-14.

[16] Deutsch R, Kudrina V, Freichel M, Grimm C. Two-pore channel regulators - Who is in control? Frontiers in Physiology. 2025; 15: 1534071. https://doi.org/10.3389/fphys.2024.1534071.

[17] Ramos I, Reich A, Wessel GM. Two-pore channels function in calcium regulation in sea star oocytes and embryos. Development (Cambridge, England). 2014; 141: 4598–4609. https://doi.org/10.1242/dev.113563.

[18] Arndt L, Castonguay J, Arlt E, Meyer D, Hassan S, Borth H, *et al*. NAADP and the two-pore channel protein 1 participate in the acrosome reaction in mammalian spermatozoa. Molecular Biology of the Cell. 2014; 25: 948–964. https://doi.org/10.1091/mbc.E13-09-0523.

[19] Oliver EI, Jabloñski M, Buffone MG, Darszon A. Two-pore channel 1 and Ca^{2+} release-activated Ca^{2+} channels contribute to the acrosomal pH-dependent intracellular Ca^{2+} increase in mouse sperm. The Journal of Physiology. 2023; 601: 2935–2958. https://doi.org/10.1113/JP284247.

[20] Sánchez-Tusie AA, Vasudevan SR, Churchill GC, Nishigaki T, Treviño CL. Characterization of NAADP-mediated calcium signaling in human spermatozoa. Biochemical and Biophysical Research Communications. 2014; 443: 531–536. https://doi.org/10.1016/j.bbrc.2013.12.011.

[21] Pitt SJ, Funnell TM, Sitsapesan M, Venturi E, Rietdorf K, Ruas M, *et al*. TPC2 is a novel NAADP-sensitive Ca^{2+} release channel, operating as a dual sensor of luminal pH and Ca^{2+}. The Journal of Biological Chemistry. 2010; 285: 35039–35046. https://doi.org/10.1074/jbc.M110.156927.

[22] Chakraborty A, Dissanayake R, Wall KA. Nicotinic Acid Adenine Dinucleotide Phosphate (NAADP)-Mediated Calcium Signaling Is Active in Memory $CD4^{+}$ T Cells. Molecules (Basel, Switzerland). 2024; 29: 907. https://doi.org/10.3390/molecules29040907.

[23] Hu W, Zeng H, Shi Y, Zhou C, Huang J, Jia L, *et al*. Single-cell transcriptome and translatome dual-omics reveals potential mechanisms of human oocyte maturation. Nature Communications. 2022; 13: 5114. https://doi.org/10.1038/s41467-022-32791-2.

[24] Pitt SJ, Reilly-O'Donnell B, Sitsapesan R. Exploring the biophysical evidence that mammalian two-pore channels are NAADP-activated calcium-permeable channels. The Journal of Physiology. 2016; 594: 4171–4179. https://doi.org/10.1113/JP270936.

[25] Trufanov SK, Rybakova EY, Avdonin PP, Tsitrina AA, Zharkikh IL, Goncharov NV, *et al*. The role of two-pore channels in norepinephrine-induced $[Ca^{2+}]i$ rise in rat aortic smooth muscle cells and aorta contraction. Cells. 2019; 8: 1144. https://doi.org/10.3390/cells8101144.

[26] Carvacho I, Lee HC, Fissore RA, Clapham DE. TRPV3 channels mediate strontium-induced mouse-egg activation. Cell Reports. 2013; 5: 1375–1386. https://doi.org/10.1016/j.celrep.2013.11.007.

[27] Krishna M, Generoso WM. Timing of sperm penetration, pronuclear formation, pronuclear DNA synthesis, and first cleavage in naturally ovulated mouse eggs. The Journal of Experimental Zoology. 1977; 202: 245–252. https://doi.org/10.1002/jez.1402020214.

[28] Publicover SJ, Giojalas LC, Teves ME, de Oliveira GSMM, Garcia AAM, Barratt CLR, *et al*. Ca^{2+} signalling in the control of motility and guidance in mammalian sperm. Frontiers in Bioscience: a Journal and Virtual Library. 2008; 13: 5623–5637. https://doi.org/10.2741/3105.

[29] Evans JP. Preventing polyspermy in mammalian eggs-Contributions of the membrane block and other mechanisms. Molecular Reproduction and Development. 2020; 87: 341–349. https://doi.org/10.1002/mrd.23331.

[30] Bianchi E, Doe B, Goulding D, Wright GJ. Juno is the egg Izumo receptor and is essential for mammalian fertilization. Nature. 2014; 508: 483–487. https://doi.org/10.1038/nature13203.

[31] Liu M. The biology and dynamics of mammalian cortical granules. Reproductive Biology and Endocrinology: RB&E. 2011; 9: 149. https://doi.org/10.1186/1477-7827-9-149.